A Journal of the Gesellschaft Deutscher Chemiker

Angewandte International Edition GDCh Chemie

www.angewandte.org

Accepted Article

Title: Iron oxidation in Escherichia coli bacterioferritin ferroxidase centre, a site designed to react rapidly with H2O2 but slowly with O2

Authors: Jacob Pullin, Michael T. Wilson, Martin Clémancey, Geneviève Blondin, Justin M. Bradley, Geoffrey R. Moore, Nick E. Le Brun, Marina Lučić, Jonathan A. R. Worrall, and Dimitri A. Svistunenko

To be cited as: *Angew. Chem. Int. Ed.* 10.1002/anie.202015964

Link to VoR: https://doi.org/10.1002/anie.202015964

WILEY-VCH

10.1002/anie.202015964

WILEY-VCH

RESEARCH ARTICLE

Iron oxidation in *Escherichia coli* bacterioferritin ferroxidase centre, a site designed to react rapidly with H_2O_2 but slowly with O_2

Jacob Pullin,[a] Michael T. Wilson,[a] Martin Clémancey,[b] Geneviève Blondin,[b] Justin M. Bradley,[c] Geoffrey R. Moore,[c] Nick E. Le Brun,[c] Marina Lučić,[a] Jonathan A. R. Worrall,[a] Dimitri A. Svistunenko*[a]

[a] Dr J. Pullin, Prof M. T. Wilson, M. Lučić, Dr J. A. R. Worrall, Dr D. A. Svistunenko
School of Life Sciences
University of Essex
Wivenhoe Park, Colchester, Essex CO4 3SQ, United Kingdom
E-mail: svist@essex.ac.ul
[b] Dr M. Clémancey, Dr G. Blondin
Université Grenoble Alpes, CNRS, CEA, IRIG
Laboratoire de Chimie et Biologie des Métaux, UMR 5249
17 rue des Martyrs, 38000 Grenoble, France
[c] Dr J. M. Bradley, Prof G. R. Moore, Prof N. E. Le Brun
School of Chemistry
University of East Anglia
Norwich Research Park Norwich, Norfolk, NR4 7TJ, United Kingdom

Supporting information for this article is given via a link at the end of the document.

Abstract: Both O_2 and H_2O_2 can oxidise iron at the ferroxidase centre (FC) of *Escherichia coli* bacterioferritin (EcBfr) but mechanistic details of the two reactions need clarification. UV-vis, EPR and Mössbauer spectroscopies have been used to follow the reactions when apo-EcBfr, pre-loaded anaerobically with Fe^{2+}, was exposed to O_2 or H_2O_2. We show that O_2 binds di-Fe^{2+} FC reversibly, two Fe^{2+} ions are oxidised in concert and a H_2O_2 molecule is formed and released to solution. This peroxide molecule further oxidises another di-Fe^{2+} FC, at a rate ~1000 faster than O_2, ensuring an overall 1:4 stoichiometry of iron oxidation by O_2. Initially formed Fe^{3+} can further react with H_2O_2 (producing protein bound radicals) but relaxes within seconds to an H_2O_2-unreactive di-Fe^{3+} form. The data obtained suggest that the primary role of EcBfr *in vivo* may be to detoxify H_2O_2 rather than sequester iron.

Introduction

Ferritins belong to the family of proteins and enzymes that exploit the chemistry of dinuclear iron complexes. The di-iron complexes embedded in proteins have many biochemical functions including catalytic organic transformation (in ribonucleotide reductases,[1] RNR, methane monoxygenases[2] and desaturases[3]) as well as reversible O_2 binding (in haemerythrins,[4] Hr). In addition to these roles, the di-iron centres in ferritins function as Fe^{2+} oxidases and iron transit sites involved in the formation of polynuclear iron minerals.[5] The oxidation of iron is coupled to reduction of O_2 (or H_2O_2) at the di-iron centres. This activity has earned them the name *ferroxidase centres* (FC).

Ferritins are typically assemblies of 24 four α-helix bundles, all or some containing a FC. One ferritin molecule can accommodate thousands of iron atoms in the central mineral core, but iron sequestering, being the primary function for some ferritins[6] is not necessarily the primary *in vivo* role of all ferritins. Acting as an antioxidant seems to be important for some, particularly in those cases when H_2O_2 appears to be the preferred oxidant.[7]

For example, the mini-ferritin Dps (DNA-binding Protein under Starvation) is a 12meric protein with dinuclear iron complex coordinated with ligands provided by both dimer subunits.[8] Dps utilises H_2O_2 rather than O_2 and is thought to protect DNA from oxidative damage under conditions of nutritional stress.[7c] This is in contrast to *E. coli* ferritin FtnA which has its primary role in iron homeostasis in metabolically active cells, and the animal H-chain ferritins – all of which prefer O_2 as the main co-substrate for Fe^{2+} oxidation.[6]

In this study, we focus on *Escherichia coli* bacterioferritin (EcBfr) for which H_2O_2 was reported to compete with O_2 very successfully in iron oxidation.[9] The rate of EcBfr-mediated iron oxidation by H_2O_2 was estimated to be 10-fold higher than by O_2.[7b] We re-evaluate this factor in this manuscript as a ~1000-fold (*vide infra*). Bacterioferritins (Bfrs) differ from other ferritins in the ligand set of their di-iron sites[10] but, most importantly, in that they can contain up to 12 haem groups at the two-fold symmetry binding sites at the interface of two subunits in twelve dimers.[11] The haem is thought to play a role in passing an electron to an iron atom in the core – for it to be reduced and released to the solution.[12] Interestingly, it appears that an electron can also be transferred from reduced Fe^{2+} haem directly to the FCs.[13]

Figure 1 illustrates the structure of the EcBfr FC when the two iron atoms are in the Fe^{2+} and Fe^{3+} oxidation states. EcBfr also has another iron binding site on the inner surface (IS) of the shell, Fe_{IS}. Replacement of the aromatic residues Tyr25, Tyr58 or Trp133, or either of the two residues coordinating the IS iron site (Figure 1C), significantly affected iron mineralisation.[14] These findings have led to the conclusion that the three aromatic residues and the Fe_{IS} site participate in the electron transfer from the ferrous iron inside the core to the ultimate oxidant (O_2).[14-15]

10.1002/anie.202015964

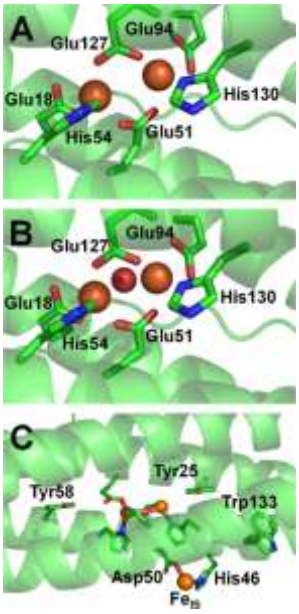

Figure 1. The ferroxidase centre (FC) of *Escherichia coli* bacterioferritin (EcBfr) in different oxidation states. **A)** The EcBfr FC with two Fe^{2+} ions bound (PDB 3E1M[14b]). **B)** Structure with Fe^{3+} ions bound at the FC (PDB 3E1N[14b]). The density between the two ferric ions was assigned to the oxygen atom of an oxo- or hydroxo-bridge connecting the two.[14b] **C)** A zoomed out view of the di-ferrous structure showing the aromatic residues thought to be involved in mineralisation[14a, 15] and the IS iron binding site coordinated by Asp50 and His46. This iron is 9.2 Å from the nearest FC iron and 10.2 Å from the second and protrudes into the central cavity. The IS iron is not observed in the di-ferric structure.[14b]

The FC's ligand arrangement in EcBfr is identical, as far as the first coordination sphere is concerned, with that in *Pseudomonas aeruginosa* BfrB,[12c] a *P. aeruginosa* Bfr (and is similar to ligand sets in RNR[1, 16] and methane monoxygenase[2a]). However, the ligand geometries in these two Bfrs are different enough to result in the very different chemistries these proteins exhibit. We have maintained the view,[5b, 5c] shared by others,[17] that a common mechanism of mineralisation in ferritins[18] does not exist, and the studies of BfrB support this view. While the FCs of EcBfr are stable and function as pure catalytic sites for O_2 reduction, the Fe^{2+} oxidation at the structurally similar BfrB FC is followed by translocation of Fe^{3+} to the interior cavity.[5d]

The stoichiometry of iron oxidation by O_2 in EcBfr was reported as 4 Fe^{2+} : 1 O_2.[9] This is not a trivial result because one O_2 molecule is extremely unlikely to oxidise 4 iron ions in 2 different FCs in a concerted reaction – there must be an intermediate(s), likely to be H_2O_2. However, attempts to quantitatively detect H_2O_2 produced during O_2-driven iron oxidations on EcBfr were only partially successful.[7b, 9] If H_2O_2 is produced, some could be lost in side reactions and not in reactions with the FCs, thus affecting the 4:1 overall stoichiometry. Such dissipation of H_2O_2, at a level of 38%, has been reported during iron oxidation by O_2 in a human heteropolymeric ferritin.[19] To further complicate matters, the Fe^{2+} : O_2 stoichiometry of iron oxidation by the human homo-24meric ferritin HuHF was reported to be 2:1,[19] not 4:1. Even as recently as last year, the stoichiometry of Fe^{2+} oxidation by O_2 in three different ferritins (two human and one horse) was considered to be as vague as either 2:1 or 4:1.[20]

Since most experiments on iron oxidation in ferritins have been performed under oxygenated conditions, when H_2O_2 might have been formed as an intermediate and contributed to overall iron oxidation, there is an urgent need to understand fully the precise chemistry through which iron is oxidised by O_2, and also by H_2O_2, and how a di-ferrous site can utilise one or the other as substrate, but avoid generating poisonous reactive oxygen species. We employed a protocol in which deoxygenated Fe^{2+}-loaded EcBfr is mixed with either oxygenated (to a controlled O_2 concentration) buffer or deoxygenated buffer containing known H_2O_2 concentrations. We used UV-vis static and stopped-flow spectrophotometry and an anaerobic Rapid Freeze-Quench (RFQ) method of making samples (45 ms - 1 min) for parallel Electron Paramagnetic Resonance (EPR) and Mössbauer spectroscopic analyses. Thus, this work provides a full account of the stoichiometries and kinetics of EcBfr-mediated iron oxidation by O_2 and by H_2O_2 and allows a comprehensive mechanism for the activity of the FC to be formulated.

Results

As the protocol employed in our investigations involves incubation of Fe^{2+} anaerobically with the apo-protein, it is prudent to re-examine the stoichiometry of Fe^{2+} binding under these conditions for comparison with the earlier approach[21] in which iron was added to aerobic solutions of apo-protein. The stoichiometries of Fe^{2+} binding to FC under anaerobic conditions (2:1) and of its oxidation thereafter by added O_2 (4:1) follow from the results reported in **Figure 2** and **Figure S1**.

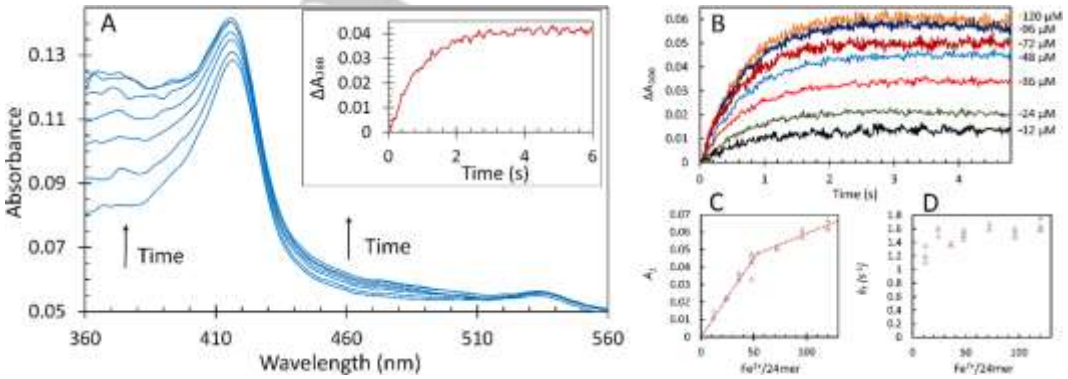

Figure 2. The fast kinetics of 1 µM apo-EcBfr pre-loaded anaerobically with Fe^{2+} and reacted with 600 µM O_2 (in 100 mM MES, pH 6.5, all concentrations are final). **A** - an example of the photodiode array (PDA) UV-vis spectra of EcBfr pre-loaded with 48 µM Fe^{2+} and mixed with O_2. The spectra correspond to the reaction times: 0.05, 0.30, 0.64, 1.03, 1.53, 2.46 and 19.68 s. The *inset* shows the time dependence of the absorbance at 380 nm increase, ΔA_{380}, associated with Fe^{2+} to Fe^{3+}

oxidation, at a resolution of 3 ms. **B** - kinetics of Fe^{2+} oxidation to Fe^{3+} (ΔA_{380}) after addition of 600 µM O_2 to 1 µM EcBfr pre-loaded with indicated concentrations of Fe^{2+} (in the mixture). Panels **C** and **D** show final absorbance A_1 and pseudo-first-order iron oxidation rate constants k_1, respectively, for the seven values of iron loading, obtained from fitting of the kinetic traces (B) with double exponent functions $\Delta A_{380} = (A_1 + A_2) - A_1 e^{-k_1 t} - A_2 e^{-k_2 t}$. The faster process ($k_1$) accounts for 90% of the overall absorbance change observed.

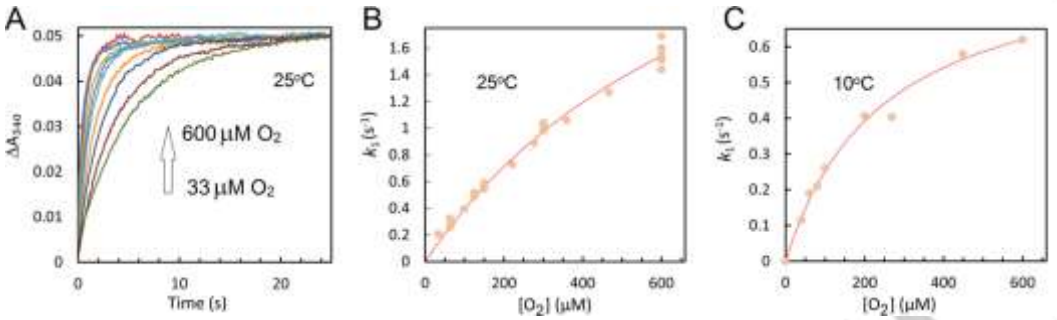

Figure 3. A – The absorbance increase, at 340 nm, as measured by the photomultiplier on addition of buffer with different concentrations of O_2 to 1 µM EcBfr anaerobically loaded with 48 µM Fe^{2+}. All traces were brought to a common endpoint of absorbance change. The data were collected at 25°C. **B** – The traces in A, as well as traces obtained in repeats, were fitted to double exponentials and the faster rate constants k_1 (circles) are plotted as function of oxygen concentration. **C** – the mixing experiments were repeated at 10°C and k_1 (circles) are plotted as function of oxygen concentration. The data in **B** and **C** were fitted to Equation 2 (lines) with parameters reported in Table S1.

The amplitude A_1 for the rapid phase of iron oxidation increases linearly with [Fe^{2+}] – up to approximately 53 Fe^{2+}/ EcBfr, which is close to the expected value of 48 for full saturation of the FCs, after which the amplitude continues to increase, but with a shallower slope (Figure 2C), and does not plateau, as in [21], due to the protocol differences. The first-order rate constant k_1 for this rapid phase is essentially independent of [Fe^{2+}] (Figure 2D) indicating that electron transfer from Fe^{2+} to O_2 in the $2Fe^{2+}$-O_2 complex in the FC is slower than O_2 binding to doubly iron-occupied FC. The linearity of the titration (Figure 2C) is consistent with cooperative binding of Fe^{2+} to the FC. Were it otherwise, the fraction of centres with two Fe^{2+} ions bound to FCs, at sub-stoichiometric [Fe^{2+}], would follow a binomial distribution and would not be linear. Cooperative binding of Co^{2+} to the FC has been reported.[22]

Consecutive additions of O_2 saturated buffer aliquots to the $(\text{apo-EcBfr} + Fe^{2+})_{\text{anaerobic}}$ system led to progressive oxidation of the Fe^{2+}, linearly with [O_2] until the point of one O_2 per 4 Fe^{2+} is reached, after which the dependence plateaus (Figure S1). Thus the stoichiometry of iron binding to and oxidation at FCs in the currently employed protocol ($(\text{apo-EcBfr} + Fe^{2+})_{\text{anaerobic}} + O_2$) is the same as in the protocol used previously ($(\text{apo-EcBfr})_{\text{aerobic}} + Fe^{2+}$).[9, 21]

Figure 3 reports the kinetics of iron oxidation as a function of O_2 concentration monitored at 340 nm. The time courses captured at 25°C (Panel A) were fitted to double exponentials (as in Figure 2, with A_1 > 90% of total ΔA) and the dependence of k_1 on [O_2], shown in panel B, is seen to be curved. This suggests O_2 binds to the Fe^{2+}-loaded FC reversibly and forms an oxy-complex in which oxidation occurs in a first order process, as shown in **Equation 1**. This mechanism yields a hyperbolic relationship between k_1 and [O_2], **Equation 2**, which we have used to fit the data in Panels B and C. The latter panel shows the data of the experiment repeated at 10°C (Panel C), where K_D is expected to be lower and thus the hyperbola more pronounced. Indeed, Figure 3C shows the hyperbolic nature of the dependence is more obvious, supporting the model of reversible O_2 binding. The values of k_1^{max} and K_D at 25°C and 10°C obtained from the fits of the data to Equation 2 are reported in **Table S1**.

$$Fe^{2+} + O_2 \underset{k_r}{\overset{k_f}{\rightleftarrows}} Fe^{2+}\cdots O_2 \xrightarrow{k_1^{max}} Fe^{3+} \qquad \text{(Eq 1)}$$

$$k_1 = \frac{k_1^{max}[O_2]}{K_D + [O_2]} \qquad \text{(Eq 2)}$$

The stoichiometry of 4:1 for iron oxidation with O_2 makes it very unlikely that four electrons are donated to one O_2 molecule in a concerted way from four Fe^{2+} ions. It is much more probable that there are steps in the reaction, first of which is oxidation of two Fe^{2+} in the FC to which O_2 is bound. This would mean that hydrogen peroxide should be formed. If so, does it stay bound to the FC or is it released into solution? To answer this question, we added Fe^{2+} to apo-EcBfr in air-equilibrated buffer that contained the dye decolourising peroxidase DtpA.[23] In the presence of H_2O_2, DtpA forms a relatively stable Compound I species, which comprises an oxo-ferryl haem and a π-cation radical on the porphyrin,[23-24] thus providing a convenient system for H_2O_2 detection and quantitation. **Figure 4** unambiguously shows that H_2O_2 is indeed formed and released to the solution on addition of iron as the DtpA optical spectrum shows changes typical of Compound I formation followed by its decay to Compound II (comprising the same oxo-ferryl haem but with the radical character now migrated away from the porphyrin). Compound I forms over ~5 s (*Inset a,* Figure 4), a time that is consistent with the time course of oxidation of the FC by O_2 (Figure 3A). The calculated spectra (**Figure S2**A) for the DtpA (Fe^{3+}) → Compound I → Compound II model are similar to the three highlighted spectra in Figure 4.

To ascertain if all or a part of the H_2O_2 formed is released to the solution, stopped-flow experiments were performed for a range of [Fe^{2+}]. Figure S2B shows that the more Fe^{2+} added, the more Compound I is formed. Based on the $\Delta\varepsilon_{390}$ ~ 30,000 M^{-1} cm^{-1} (for the absorbance difference $A_{390}^{ferric\ DtpA} - A_{390}^{Compound\ I}$) determined from the published spectra,[24b] the concentrations of Compound I at each iron loading have been calculated and are reported in *Inset b*, Figure 4. The yield of Compound I formed in the DtpA+apo-EcBfr system is directly proportional to the amount of ferrous iron added – up to the concentration required to

completely fill all FCs, when Compound I is formed at a high yield of ~6 µM – a half of a possible maximum of ~12 µM. This indicates that the second-order rate constant of FC (doubly filled with Fe^{2+}) reacting with H_2O_2 must be comparable with that of DtpA reacting with H_2O_2 (8.9 ± 0.25 ×10^6 M^{-1} s^{-1} at pH 7[24b] and 1.4 x 10^7 $M^{-1}s^{-1}$ at pH 6.5 (this work, not shown)).

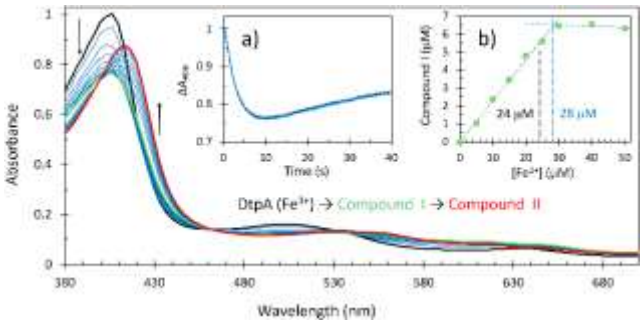

Figure 4. The PDA UV-vis spectra of 18 µM DtpA in an oxygenated solution of 0.5 µM apo-EcBfr as it is mixed with 50 µM iron (100 Fe^{2+}/24mer). The selected spectra shown are taken at the time points ranging from 40 ms (black spectrum) to 40 s (red spectrum). The spectrum in green corresponds to 9.27 s. *Inset a* shows the absorbance change in the Soret band (at 406 nm) associated with formation of Compound I and its later decay to Compound II. *Inset b* shows formation of Compound I as function of [Fe^{2+}] added (see Figure S2B). The first six and the last three data points have been fitted with straight lines, their intercept resulting in [Fe^{2+}] = 28 µM which is close to the theoretical value of 24 µM of iron load when all FCs are expected to be occupied with iron.

Thus, H_2O_2 is an important player in the FC iron oxidation by O_2. The stoichiometry of Fe^{2+} to Fe^{3+} oxidation by H_2O_2 in the ((apo-EcBfr + Fe^{2+})$_{anaerobic}$ + H_2O_2) system was studied and confirmed to be one peroxide to two Fe^{2+} (**Figure S3).**

The stopped-flow PDA UV-vis spectra of H_2O_2 reacting with 48 Fe^{2+}/24mer EcBfr are shown in **Figure S4**A. The noisy time course at 380 nm (*inset*) cannot be used to determine the rate constant of the oxidation accurately. Therefore, we used a photomultiplier that has a much higher time resolution and also can be used at 340 nm, a wavelength used in previous studies.[15, 25]

Figure 5A shows the time courses of iron oxidation by H_2O_2 in the anaerobically prepared Fe^{2+}-EcBfr complex. Those comprise a fast phase and further slower processes - fitted by the triple exponent function given in **Equation 3**.

$$\Delta A_{340} = (A_1 + A_2 + A_3) - A_1 e^{-k_1 t} - A_2 e^{-k_2 t} - A_3 e^{-k_3 t} \quad \text{(Eq 3)}$$

The fastest process shows a linear dependence of its pseudo-first-order rate constant k_1 on [H_2O_2] (Figure 5B), yielding a second-order rate constant of 3.76 x 10^6 M^{-1} s^{-1}. Thus for comparable concentrations of H_2O_2 and O_2, the rate of iron oxidation by peroxide is ~1000 times higher than by O_2 (cf. Figure 5B & Figure 3B). Identical data were obtained for four variants (Figure 5B) in which phenylalanine substituted for aromatic residues previously implicated in iron mineralisation.[14a, 15] The data for the two much slower processes (**Figure S5**A and Figure S5B) are scattered and will be discussed later.

In Figure 5C, the amplitude of the fast phase (A_1) of the reaction is shown as a function of [H_2O_2], from sub- to supra-stoichiometric concentrations (with a reference to **Figure S6**), and is seen to increase until sufficient [H_2O_2] is present to oxidise all iron in the FCs after which a plateau is reached, showing that H_2O_2 is fully consumed in this reaction.

We have previously reported protein radical formation in the (apo-EcBfr)$_{aerobic}$ + Fe^{2+} system with Tyr25 being the principal site.[15] The rate of Tyr25 radical decay coincides with the rate of a secondary radical(s) formation, and Tyr58 and Trp133 have been shown to be involved in the overall process of radical dissipation.[14a] Having established that H_2O_2 reacts with EcBfr anaerobically loaded with Fe^{2+} more than 1000 times faster than O_2, it is important to determine if H_2O_2 leads to protein radicals formation when added to the (apo-EcBfr + Fe^{2+})$_{anaerobic}$ system. **Figure S7** shows that, indeed, free radicals are formed. A comparison of spectra A and B in Figure S7 shows that 250 µM H_2O_2 (a slight stoichiometric excess enough to oxidise 250 µM x 2 = 500 µM Fe^{2+} whilst only 400 µM Fe^{2+} are present) yields, a few seconds after mixing, ~40 times more free radicals than ambient oxygen (sufficient to oxidise 260 µM x 4 = 1040 µM Fe^{2+}) when oxidising the same 500 µM Fe^{2+}. Spectra B and C, on the other hand, show that the same concentration of H_2O_2 produces far fewer free radicals if it is sub-stoichiometric to iron – enough to oxidise 500 µM Fe^{2+} whilst the ferrous iron concentration is 1200 µM.

Thus, when O_2 or H_2O_2 oxidises ferrous ions at FCs, no oxidation equivalents are available to produce free radicals on EcBfr. One way to explain the experimentally observed radicals in O_2- and H_2O_2-treated proteins is to suggest that H_2O_2 reacts with di-ferric FCs. This should result in further oxidation of iron transiently bringing it to a ferryl oxidation state. Its subsequent fast reduction to the ferric state would cause formation of free radicals on protein amino acid residue(s). We now enquire if ferryl iron in the FC can be detected.

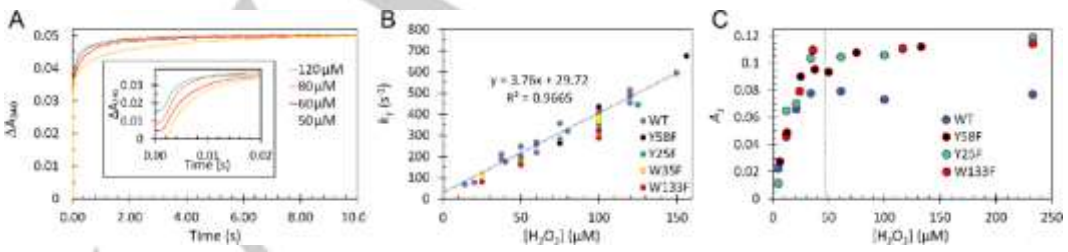

Figure 5. Kinetics of iron oxidation in the FC by H_2O_2. **A.** Four examplary kinetics of absorbance increase at 340 nm on mixing wild type (WT) apo-EcBfr (1 µM after mixing) anaerobically loaded with Fe^{2+} (48 µM after mixing) with buffer containing H_2O_2 (concentrations after mixing indicated). Each trace represents an average of three mixing experiments. All traces were brought to a common endpoint (at 10 s). The *inset* shows the initial 20 ms of the time courses, corresponding to the fast phase of the reaction. **B.** The values of k_1 obtained from fitting the 340 nm kinetics in the WT and the four EcBfr variants to Equation 3, plotted versus [H_2O_2]. **C.** The amplitude of the fast phase (A_1, see Equation 3) as a function of [H_2O_2] for 2 µM apo-EcBfr anaerobically loaded with 96 µM Fe^{2+}]; the stoichiometric [H_2O_2] indicated, 48 µM.

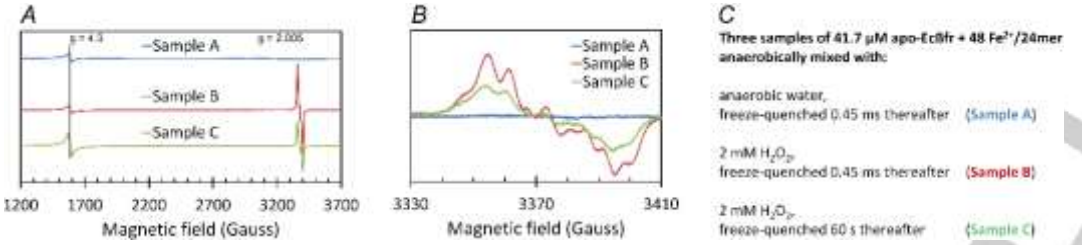

Figure 6. EPR spectra of the RFQ Samples A, B and C prepared as detailed in Experimental Procedures, 1.8, and taken at 23 K. ***A*** - overall spectra covering the signals from the rhombic ferric iron at g=4.3 and the free radicals at g = 2.005 (the default instrumental parameters were altered as follows: P_{MW} = 3.18 mW, Am = 5 G, V = 22.6 G s^{-1}). ***B*** - detailed free radical EPR region. ***C*** – the details of samples A, B and C (see Experimental Procedures, 1.8).

We used a new methodology of making anaerobic RFQ samples for parallel EPR and Mössbauer spectroscopy analysis (Experimental Procedures, 1.7-1.8). The EPR and Mössbauer spectra of the samples are reported in **Figure 6** and **Figure S8**, respectively.

The control Sample A (ferrous as prepared) shows in the EPR spectrum no free radical and a g=4.3 EPR signal from rhombic ferric iron which is a sum of the background signal (from the quartz assembly) and residual ferric iron associated with apo-EcBfr (as prepared at a rather high concentration of the FC, 2 mM). The Mössbauer spectrum of Sample A (Figure S8) exhibits two lines close to –0.3 and +2.9 mm s^{-1} and has been simulated as either one or a superposition of two doublets (**Figure S9, Table S2)**, both cases consistent with high-spin ferrous ions.[7d, 26]

A strong free radical EPR signal is recorded in Sample B, while the g=4.3 signal is not affected at this time point of the reaction (45 ms, Figure 6). An assessment of the concentration of the free radicals shows it is still a small fraction (~5-15%) of the FC concentrations. The very same line shape free radical EPR spectrum but half the intensity is seen 60 s after the reaction starts, and the g = 4.3 signal is increased (Sample C, Figure 6). Our detailed study of the nature of free radicals formed in EcBfr treated with H_2O_2 will be reported elsewhere.

The high velocity line of the ferrous doublet (red dashed line, Figure S8) is not present in the Mössbauer spectra of the H_2O_2-treated samples (B and C) suggesting that all the Fe^{2+} sites are oxidised. The main features in these spectra (Figure S8) are found within the narrow interval of –1 to 2.3 mm s^{-1}. To better characterise the species responsible, and to investigate if they are different at 45 ms and 1 min after H_2O_2 addition, samples B and C were recorded at a narrower velocity window - ±3 mm s^{-1} (at 60 mT) thus providing a better resolution and clear evidence that the iron states differ between 45 ms and 1 min freezing time (**Figure S10**).

To further investigate these differences, the Mössbauer spectra of Samples B and C were recorded at a greater magnetic field – 7 T parallel to the γ-ray. The spectra of the 45 ms sample measured at 60 mT and 7 T have been simulated as sums of spectra from four ferric sites (**Figure 7**A). The absence of the

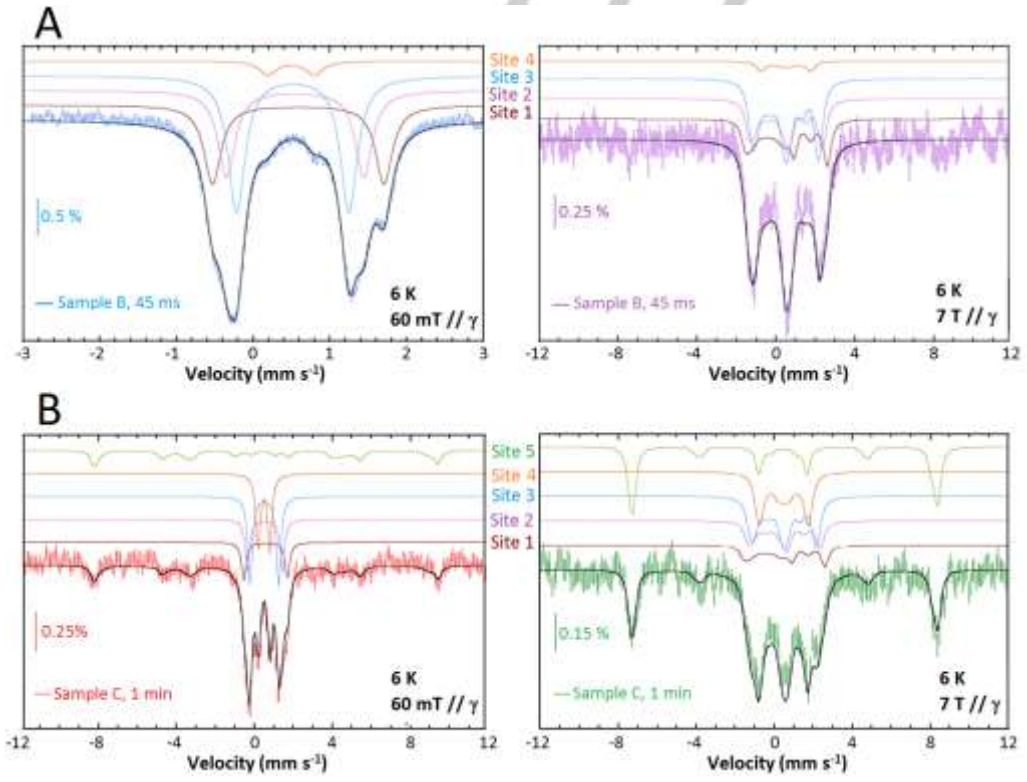

Figure 7. The Mössbauer spectra of EcBfr treated with H_2O_2 and frozen 45 ms and 1 min thereafter (Sample B and Sample C, respectively) measured at 60 mT and 7 T of magnetic field, parallel to the γ-ray path. **A** – Sample B (45 ms) spectra are simulated as sums of four ferric sites. **B** – Sample C (1 min) spectra are simulated as sums of the same four sites (at a different proportion), plus one more ferric site, Site 5. The latter Site 5 is paramagnetic which is evidenced from both 60 mT and 7 T spectra. The experimental spectra were measured at 6 K. The simulated spectra were all constrained to the same line width, 0.27 mm/s. Simulation parameters are given in **Table S3**.

hyperfine splitting at the higher magnetic field and wider velocity window indicates that all ferric iron species are antiferromagnetically coupled thus producing no paramagnetism.

Sample C (frozen 1 min after H_2O_2 addition) exhibits 60 mT and 7 T Mössbauer spectra that can be represented as sums of the same four spectra simulated for the 45 ms sample (see Figure 7A), though in a different combination, plus one more spectrum (Site 5) with the hyperfine features spreading over an interval of ~± 9 mm s^{-1} indicating the site is paramagnetic (Figure 7B). The appearance of this paramagnetic ferric species in the Mössbauer spectrum of the 1 min sample is fairly consistent with the increased intensity of the g = 4.3 signal from the S=5/2 species detected by the EPR spectroscopy in the same sample (Figure 6). The correlation between Site 5 content and the concentration of the species responsible for the g= 4.3 EPR signal is not quantitatively consistent, as far as the data obtained are concerned, and requires further investigation to be statistically confirmed. The intensity of the g = 4.3 EPR signal is too low for a g = 9.7 component of the EPR spectrum of high spin Fe^{3+} in rhombic ligand field[27] to be detectable over the noise level – the area covering this g-value was monitored in the EPR spectra (from 600 G) but showed a flat line and is not included in Figure 6.

None of the simulated line shapes proposed to contribute to the Mössbauer spectra at 45 ms and 1 min can be linked to a ferryl iron state. This is in contrast to the previous report of $^{57}Fe^{4+}$ signature in *Pyrococcus furiosus* ferritin (PfFtn), albeit at a low yield of 5±2% of total ^{57}Fe.[28]

Discussion

The proposed mechanism of iron oxidation at the FC is presented in **Figure 8** and comprises three sets of reactions, A, B and C.

Pathway A depicts the reactions of a di-ferrous FC with O_2. Oxygen binds rapidly but weakly. At ambient [O_2], taking K_D = 823 μM, only ~24% of the EcBfr FCs are at any time in the oxy form. At lower [O_2], likely to be found in the cytoplasm of *E. coli* in its natural environment, the oxy form will be very poorly populated and oxidation of the iron would be extremely slow.

We propose that O_2 binds to EcBfr in a way similar to Hr - to one of the two iron atoms,[29] Deoxy di-ferrous Hr has a bridging water (or a hydroxyl group) implicated in such binding[29] but di-ferrous EcBfr, in contrast, does not show such density in the X-ray structure[14b] We think, however, it is possible that the cluster of three water molecules near the FC iron coordinated by His130, plus a water molecule close to the other iron of the FC (Supporting Information file *Three plus one waters above FC in EcBfr.pdb*), may be rearranged by in-coming O_2 to form a bridge between the two iron atoms as hypothesised in Figure 8. The Hr type O_2 binding to the di-ferrous centre[29-30] has been subjected to theoretical modelling and has been shown to account well for reversible O_2 binding in Hr.[31] EcBfr, we suggest, may be considered qualitatively similar to Hr but quantitatively different,

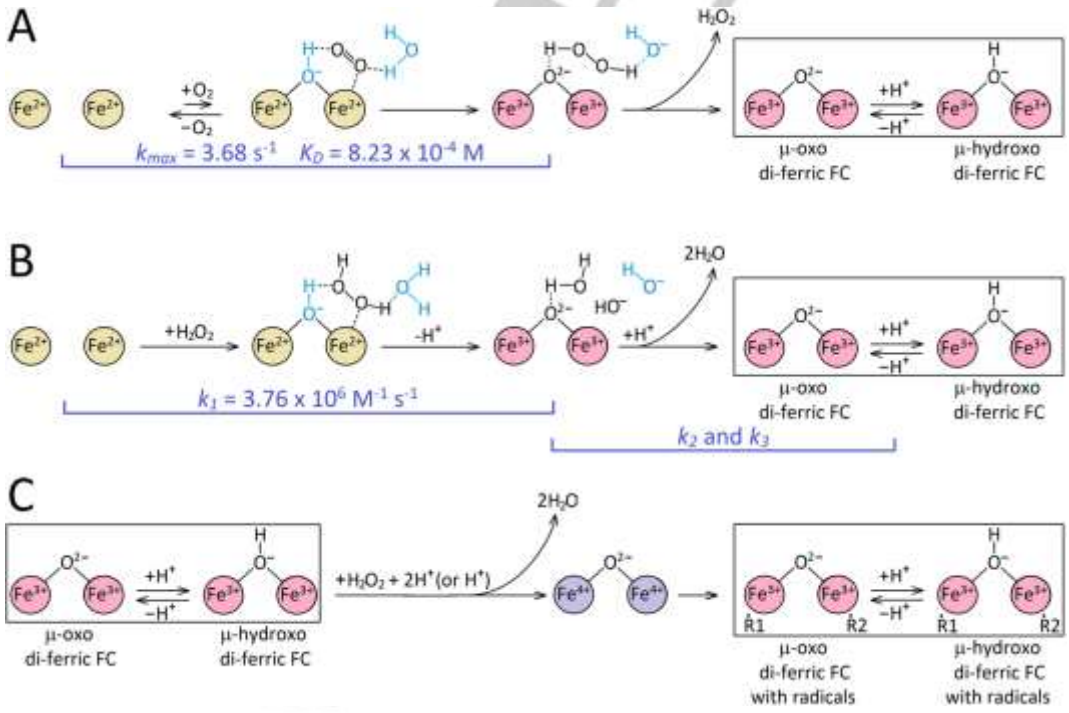

Figure 8. The three sets of reactions of iron oxidation at the FC of EcBfr – by O_2 (A), by H_2O_2 (B) and the reaction of the oxidised (di-ferric) FC with H_2O_2 (C) leading to free radical formation. We put forward the hypothesis that both O_2 and H_2O_2 bind to one of the two iron atoms which must be facilitated by structural water and/or hydroxyls (shown in blue colour) or a nearby residue(s), such as Glu94, that provide hydrogen bonding to O_2 and H_2O_2.

having a higher K_D and a much larger 'autoxidation' rate constant. An alternative mode of O_2 binding, in which O_2 bridges between the iron atoms, leads to rapid electron transfer yielding a peroxo-bridged di-ferric centre from which O_2 cannot dissociate (see, for example [32]).

Two electrons transferred from the di-ferrous FC to O_2 yield an H_2O_2 molecule, which is released to solution (Figure 4). Its reaction path with another FC is given in Figure 8B.

Pathway B. The H_2O_2 binding is rapid and proposed to be to one iron, similar to O_2 binding, with stabilising hydrogen bonds provided by the water cluster.

Iron oxidation by H_2O_2 is much faster than by O_2. Although noisy, the spectra in Figure S4A and the way they are changing in time are very similar to those in Fe^{2+} oxidation by oxygen (Figure 2A) and in titration of ferrous EcBfr with either O_2 (Figure S1) or H_2O_2 (Figure S3). The Singular Value Decomposition[33] (SVD) analysis of the complete PDA spectral set also yields two spectral components consistent with the EcBfr(Fe^{2+}) to EcBfr(Fe^{3+}) transition (Figure S4B). This means that O_2 and H_2O_2 driven oxidation of iron in the FC, while being three orders of magnitude different in rate, produce essentially the same spectral changes both at the earliest stage of reaction and minutes later, for the final products of oxidation.

The second-order rate constant of iron oxidation by H_2O_2, 3.76 x 10^6 M^{-1} s^{-1} (Figure 8B, Figure 5B), is only ~2 fold lower than the constant of peroxide reacting with DtpA, a peroxidase for which H_2O_2 is a designated substrate, k = 8.9 ± 0.25 ×10^6 M^{-1} s^{-1}.[24b] We emphasise that it is this very high rate constant than warrants the 4:1 stoichiometry of iron oxidation by O_2 (Figure S1) - every molecule of H_2O_2 formed in one FC oxidation by an O_2 is used to oxidise ferrous iron in other FCs.

Interestingly, replacement, with phenylalanine, of the aromatic residues (Figure 5, Figure S5) implicated in iron mineralisation by EcBfr,[14a, 15] had no effect on the rate constants of iron oxidation. Therefore, H_2O_2 binding to di-ferrous FC and its oxidation to the di-ferric state is unlikely to involve any redox chemistry of the aromatic residues surrounding the FC.

Kinetics of iron oxidation by sub- and supra-stoichiometric [H_2O_2] show that the amplitude (A_1) of the fastest process (k_1) is directly proportional to [H_2O_2] up to the value required for oxidation of all iron bound to the FCs (Figure 5C). This result allows the conclusion that all iron is oxidised in the first, fastest phase of absorbance change (~20 ms). As the phase associated with k_2 does not appear until [H_2O_2] is in excess (Figure S6), we may assign this process to a second-order reaction of the excess peroxide with the di-ferric centres generated in the first, fast, process (see Pathway C below). Further, k_3 has no discernible dependence on [H_2O_2] and is present at both sub- and supra-stoichiometric [H_2O_2]. This process therefore cannot be associated with electron transfer (oxidation/reduction) – it is much slower than processes 1 and 2 and the only reasonable explanation for it is that it is associated with some structural changes in molecular arrangement. The time scale of these changes is consistent with the process that takes place in the time span 45 ms – 1 min as observed in the Mössbauer spectroscopy experiments. We therefore assign this phase to the configurational changes of the FC following its oxidation to the di-ferric state.

Our conclusions that all iron is oxidised during the fastest phase and that the slower two phases are associated with configurational changes and side reactions with excess H_2O_2 are supported by the Mössbauer spectroscopy data.

Without H_2O_2, most of ^{57}Fe remains in the ferrous state (Figure S9). The EcBfr samples freeze-quenched 45 ms and 1 min after H_2O_2 addition show no ferrous iron remained in the FC (Figure S8). Neither ferryl species are found (Figure 7) which should have significantly smaller values of the isomer shift[34] than those used to simulate the five spectra for the Sites 1-5 (Table S3). On the contrary, the simulation parameters of all five sites identified in the H_2O_2–treated samples are consistent with ferric species.[35]

All four iron sites identified in the 45 ms sample are diamagnetic. This means that, at this time point, two ferric ions in every FC remain antiferromagnetically coupled. The contributions of Sites 1 and 2 are almost identical (27-29%, Table S3), suggesting that these sites belong to the same FC (*dissymmetrical* FC). Their isomer shifts (Table S3) are at the higher limit of the range for ferric ions. This is usually observed for peroxodiferric intermediates.[34, 36] Two ferric ions (also coupled) in the *symmetrical* di-ferric FC (giving identical Mössbauer signatures - Site 3, Figure 7, **Figure S11**) contribute most to the overall spectrum (~46%, Table S3). We propose that the two di-ferric FCs, dissymmetrical (Site 1 – Site 2) and symmetrical (Site 3 – Site 3), differ in immediate coordination of one of the iron ions. We propose that the (Site 1 – Site 2) FC is a peroxodiferric FC in which the peroxo group is bound to one of the two iron ions whereas the two are linked with a μ-oxo bridge, similarly to the peroxodiferric centre in Hr.[29, 34] The (Site 3 – Site 3) FC, on the other hand, does not have this peroxo ligand to one of the ions and shows typical[35a] μ-oxo di-ferric (symmetrical) Mössbauer parameters (Figure S11).

All four sites in the 45 ms sample are found in changed proportions in the 1 min sample - Sites 1-3 decrease while Site 4 contribution increases from 5% to 23% (Table S3). The isomer shift of Site 4 is close to those of the μ-oxo species, but its quadrupole splitting is significantly lower which is consistent with a di-ferric μ-hydroxo species.[35a, 35c, 37] We propose therefore that Site 4 is formed via protonation of Site 3 (μ-oxo di-ferric to μ-hydroxo di-ferric Figure S11).

Along with Site 4, another species emerges over the 45 ms – 1 min interval - a paramagnetic Site 5 with well-defined parameters of a high-spin (S=5/2) monomeric iron site. This is evidenced by both the 60 mT and 7 T Mössbauer experiments (Figure 7B) and supported by the increased g=4.3 EPR signal at 1 min (Figure 6).

In reaction set C (**Pathway C,** Figure 8), we propose a mechanism for free radical formation on EcBfr – it can only be explained by the reaction of H_2O_2 with oxidised FC already formed. A likely possibility is that one H_2O_2 molecule binds to a 'freshly' oxidised FC and takes two electrons, in a rapid succession or in concert, from the two ferric ions, thus forming a di-ferryl ($2Fe^{4+}$) state. The two ferryl ions are re-reduced by two different protein residues, thus forming two different protein-based radicals and returning the FC to the di-ferric state. (We will report elsewhere that indeed more than one primary radical is formed on EcBfr

under excess of H_2O_2). These redox processes, and the conformation/coordination changes that follow, take place over a much longer time scale than primary Fe^{2+}→Fe^{3+} oxidation and must be associated with the slower kinetic phases (with rate constants k_2 and k_3) of the absorbance increase (Figure S5, Figure S6).

The need to postulate a 'freshly' oxidised FC follows from the experimental fact that H_2O_2 does not produce any radical if added to an EcBfr sample fully loaded with iron and oxidised to a di-ferric state a few minutes earlier. This means that the 'relaxed' oxidised FC cannot react with H_2O_2, while just oxidised but not 'relaxed' FC can. In terms of the iron sites identified from the Mössbauer spectra, the 'freshly' oxidised FC are Sites 1, 2 and 3 (all three seen in the 45 ms sample) and the 'relaxed' oxidised FC is associated with sites 4 and 5 (elevated over 45 ms – 1 min, while sites 1, 2 and 3 decreased).

Thus, we propose that μ-oxo bridged di-ferric state forms first and then is protonated (Figure S11). This hypothesis requires further investigation. It is likely that once the μ-hydroxo state is formed, further re-arrangements of the ligands can occur, leading to two unbridged ferric atoms which are now uncoupled, showing paramagnetism and also unavailable for reacting with H_2O_2 (Figure S11).

Conclusions

1) Oxygen binds reversibly and weakly (K_D = 823 μM) to the di-Fe^{2+} site to form an oxy-complex in which electron transfer takes place, forming H_2O_2 that dissociates rapidly and fully into solution.
2) Released peroxide reacts very rapidly (k = 3.76 x 10^6 $M^{-1}s^{-1}$) and quantitatively with remaining di-Fe^{2+} sites accounting for the 2 Fe^{2+} : 1 H_2O_2 and the 4 Fe^{2+} : 1 O_2 stoichiometries.
3) Both oxidising equivalents of peroxide are delivered to the di-Fe^{2+} site in the ms time range converting it to the μ-oxo di-Fe^{3+} form. No radicals can be formed in this oxidation process. Over tens of seconds, it evolves into protonated, μ-hydroxo di-Fe^{3+} form.
4) Excess peroxide reacts with di-Fe^{3+}, to yield protein-based radicals. We propose a hypothesis that that H_2O_2 reacts only with the μ-oxo and not the μ-hydroxo bridged di-ferric ions.

This mechanism shows that at low oxygen concentrations, as may be experienced by *E. coli* in its natural environment, the di-ferrous iron in the FC is oxidised extremely slowly by O_2 while oxidation by H_2O_2 is at least 1000-fold faster. This supports the suggestion that one role of EcBfr may be to act as part of an antioxidant defence system, rapidly sequestering and rendering harmless peroxide in the cellular environment.

Acknowledgements

This work was supported by the United Kingdom's Biotechnology and Biological Sciences Research Council through grants BB/R002363/1 and BB/R003203/1. ML is the recipient of a Peter Nicholls PhD Scholarship. MC and GB thank the Labex ARCANE and CBH-EUR-GS (ANR-17-EURE-0003) for partial funding. We thank Radu Silaghi-Dumitrescu for useful discussion of possible modes of O_2 binding to di-iron centres.

Keywords:

E. coli EcBfr • EPR spectroscopy • fast kinetics • ferritins • ferroxidase centre • metalloproteins • Mössbauer spectroscopy • oxidation • peroxidases • radical reactions • rapid freeze-quenching • RFQ • stopped-flow spectrophotometry •

References

[1] a) P. Nordlund, B. M. Sjoberg, H. Eklund, *Nature* **1990**, *345*, 593-598; b) P. Nordlund, H. Eklund, *J. Mol. Biol.* **1993**, *232*, 123-164.
[2] a) A. C. Rosenzweig, C. A. Frederick, S. J. Lippard, P. Nordlund, *Nature* **1993**, *366*, 537-543; b) C. E. Tinberg, S. J. Lippard, *Acc. Chem. Res.* **2011**, *44*, 280-288.
[3] a) J. A. Broadwater, J. A. Haas, B. G. Fox, *Fett/Lipid* **1998**, *100* 103–113; b) J. Shanklin, J. E. Guy, G. Mishra, Y. Lindqvist, *J. Biol. Chem.* **2009**, *284*, 18559-18563.
[4] a) M. A. Holmes, R. E. Stenkamp, *J. Mol. Biol.* **1991**, *220*, 723-737; b) S. Sheriff, W. A. Hendrickson, J. L. Smith, *J. Mol. Biol.* **1987**, *197*, 273-296; c) R. E. Stenkamp, L. C. Sieker, L. M. Jensen, *J. Am. Chem. Soc.* **1984**, *106*, 618-622.
[5] a) E. C. Theil, *Annu. Rev. Biochem.* **1987**, *56*, 289-315; b) J. M. Bradley, N. E. Le Brun, G. R. Moore, *J. Biol. Inorg. Chem.* **2016**, *21*, 13-28; c) J. M. Bradley, G. R. Moore, N. E. Le Brun, *J. Biol. Inorg. Chem.* **2014**, *19*, 775-785; d) M. Rivera, *Acc. Chem. Res.* **2017**, *50*, 331-340.
[6] H. Abdul-Tehrani, A. J. Hudson, Y. S. Chang, A. R. Timms, C. Hawkins, J. M. Williams, P. M. Harrison, J. R. Guest, S. C. Andrews, *J. Bacteriol.* **1999**, *181*, 1415-1428.
[7] a) T. Haikarainen, A. C. Papageorgiou, *Cell Mol. Life Sci.* **2010**, *67*, 341-351; b) F. Bou-Abdallah, A. C. Lewin, N. E. Le Brun, G. R. Moore, N. D. Chasteen, *J. Biol. Chem.* **2002**, *277*, 37064-37069; c) E. C. Theil, *Inorg. Chem.* **2013**, *52*, 12223-12233; d) C. G. Timoteo, M. Guilherme, D. Penas, F. Folgosa, P. Tavares, A. S. Pereira, *Biochem. J.* **2012**, *446*, 125-133.
[8] S. Roy, S. Gupta, S. Das, K. Sekar, D. Chatterji, M. Vijayan, *J. Mol. Biol.* **2004**, *339*, 1103-1113.
[9] X. Yang, N. E. Le Brun, A. J. Thomson, G. R. Moore, N. D. Chasteen, *Biochemistry* **2000**, *39*, 4915-4923.
[10] S. C. Andrews, J. M. Smith, S. J. Yewdall, J. R. Guest, P. M. Harrison, *FEBS Lett.* **1991**, *293*, 164-168.
[11] F. Frolow, A. J. Kalb, J. Yariv, *Nat. Struct. Biol.* **1994**, *1*, 453-460.
[12] a) S. K. Weeratunga, C. E. Gee, S. Lovell, Y. Zeng, C. L. Woodin, M. Rivera, *Biochemistry* **2009**, *48*, 7420-7431; b) H. Yao, Y. Wang, S. Lovell, R. Kumar, A. M. Ruvinsky, K. P. Battaile, I. A. Vakser, M. Rivera, *J. Am. Chem. Soc.* **2012**, *134*, 13470-13481; c) Y. Wang, H. Yao, Y. Cheng, S. Lovell, K. P. Battaile, C. R. Midaugh, M. Rivera, *Biochemistry* **2015**, *54*, 6162-6175; d) A. N. D. Punchi Hewage, H. Yao, B. Nammalwar, K. K. Gnanasekaran, S. Lovell, R. A. Bunce, K. Eshelman, S. M. Phaniraj, M. M. Lee, B. R. Peterson, K. P. Battaile, A. B. Reitz, M. Rivera, *J. Am. Chem. Soc.* **2019**, *141*, 8171-8184.
[13] J. Pullin, M. T. Wilson, J. M. Bradley, G. R. Moore, N. E. Le Brun, D. A. Svistunenko, *Submitted to Angew Chem Int Ed* **2020**.
[14] a) J. M. Bradley, D. A. Svistunenko, G. R. Moore, N. E. Le Brun, *Metallomics* **2017**, *9*, 1421-1428; b) A. Crow, T. L. Lawson, A. Lewin, G. R. Moore, N. E. Le Brun, *J. Am. Chem. Soc.* **2009**, *131*, 6808-6813.
[15] J. M. Bradley, D. A. Svistunenko, T. L. Lawson, A. M. Hemmings, G. R. Moore, N. E. Le Brun, *Angew. Chem. Int. Ed. Engl.* **2015**, *54*, 14763–14767.
[16] M. Hogbom, M. Galander, M. Andersson, M. Kolberg, W. Hofbauer, G. Lassmann, P. Nordlund, F. Lendzian, *Proc. Natl. Acad. Sci. U. S. A.* **2003**, *100*, 3209-3214.
[17] Y. Kwak, J. K. Schwartz, V. W. Huang, E. Boice, D. M. Kurtz, Jr., E. I. Solomon, *Biochemistry* **2015**, *54*, 7010-7018.
[18] K. Honarmand Ebrahimi, P. L. Hagedoorn, W. R. Hagen, *Chem. Rev.* **2015**, *115*, 295-326.
[19] M. Mehlenbacher, M. Poli, P. Arosio, P. Santambrogio, S. Levi, N. D. Chasteen, F. Bou-Abdallah, *Biochemistry* **2017**, *56*, 3900-3912.
[20] F. Bou-Abdallah, N. Flint, T. Wilkinson, S. Salim, A. K. Srivastava, M. Poli, P. Arosio, A. Melman, *Metallomics* **2019**, *11*, 774-783.
[21] N. E. Le Brun, M. T. Wilson, S. C. Andrews, J. R. Guest, P. M. Harrison, A. J. Thomson, G. R. Moore, *FEBS Lett.* **1993**, *333*, 197-202.
[22] A. M. Keech, N. E. Le Brun, M. T. Wilson, S. C. Andrews, G. R. Moore, A. J. Thomson, *J. Biol. Chem.* **1997**, *272*, 422-429.
[23] M. L. Petrus, E. Vijgenboom, A. K. Chaplin, J. A. Worrall, G. P. van Wezel, D. Claessen, *Open Biol.* **2016**, *6*, 150149.
[24] a) A. K. Chaplin, T. M. Chicano, B. V. Hampshire, M. T. Wilson, M. A. Hough, D. A. Svistunenko, J. A. R. Worrall, *Chemistry* **2019**, *25*, 6141-6153; b) A. K. Chaplin, M. T. Wilson, J. A. R. Worrall, *Dalton Trans.* **2017**, *46*, 9420-9429.
[25] S. G. Wong, R. Abdulqadir, N. E. Le Brun, G. R. Moore, A. G. Mauk, *Biochem. J.* **2012**, *444*, 553-560.

[26] a) J. B. Lynch, C. Juarez-Garcia, E. Munck, L. Que, Jr., *J. Biol. Chem.* **1989**, *264*, 8091-8096; b) B. G. Fox, M. P. Hendrich, K. K. Surerus, K. K. Andenson, W. A. Froland, J. D. Lipscomb, E. Munck, *J. Am. Chem. Soc.* **1993**, *115*, 3688-3701; c) R. Banerjee, K. K. Meier, E. Munck, J. D. Lipscomb, *Biochemistry* **2013**, *52*, 4331-4342.
[27] M. I. Scullane, L. K. White, N. D. Chasteen, *J Magn Reson* **1982**, *47*, 383-397.
[28] K. Honarmand Ebrahimi, E. Bill, P. L. Hagedoorn, W. R. Hagen, *FEBS Lett.* **2017**, *591*, 1712-1719.
[29] M. A. Holmes, I. Le Trong, S. Turley, L. C. Sieker, R. E. Stenkamp, *J. Mol. Biol.* **1991**, *218*, 583-593.
[30] R. E. Stenkamp, *Chem. Rev.* **1994**, *94*, 715-726.
[31] a) M. Wirstam, S. J. Lippard, R. A. Friesner, *J. Am. Chem. Soc.* **2003**, *125*, 3980-3987; b) T. Brunold, C. , E. I. Solomon, *J. Am. Chem. Soc.* **1999**, *121*, 8288-8295.
[32] M. A. Cranswick, K. K. Meier, X. Shan, A. Stubna, J. Kaizer, M. P. Mehn, E. Munck, L. Que, Jr., *Inorg. Chem.* **2012**, *51*, 10417-10426.
[33] G. H. Golub, C. F. Van Loan, *Matrix Computations*, 2nd ed. ed., Johns Hopkins University Press, Baltimore, **1989**.
[34] A. J. Jasniewski, L. Que, Jr., *Chem. Rev.* **2018**, *118*, 2554-2592.
[35] a) D. M. Kurtz, Jr., *Chem. Rev.* **1990**, *4*, 585-606; b) B. Wörsdörfer, D. A. Conner, K. Yokoyama, J. Livada, M. Seyedsayamdost, W. Jiang, A. Silakov, J. Stubbe, J. M. Bollinger, Jr., C. Krebs, *J. Am. Chem. Soc.* **2013**, *135*, 8585-8593; c) C. Mathevon, F. Pierrel, J. L. Oddou, R. Garcia-Serres, G. Blondin, J. M. Latour, S. Menage, S. Gambarelli, M. Fontecave, M. Atta, *Proc. Natl. Acad. Sci. U. S. A.* **2007**, *104*, 13295-13300.
[36] A. Trehoux, J.-P. Mahy, F. Avenier, *Coord. Chem. Rev.* **2016**, *322*, 142-158.
[37] L. Shu, J. A. Broadwater, C. Achim, B. G. Fox, E. Münck, J. L. Que, . *J. Biol. Inorg. Chem.* **1998**, *3*, 392-400.

10.1002/anie.202015964

WILEY-VCH

RESEARCH ARTICLE

Entry for the Table of Contents

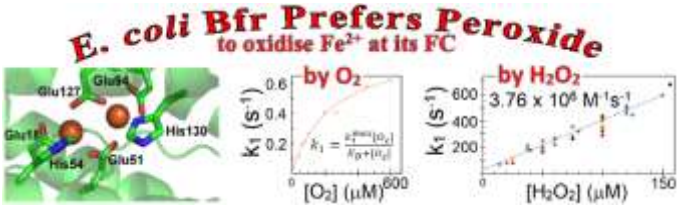

The kinetics of *E. coli* bacterioferritin di-ferrous ferroxidase centre reacting with O_2 and H_2O_2 shows that H_2O_2 reacts ~1000 times faster than O_2 implying that the primary *in vivo* role of the protein is ROS detoxification rather than iron sequestering.

Institute and/or researcher Twitter usernames: @JustinB11698455, @Nick_Le_Brun, @jarworrall, @epr_essex